Atmospheric Environment 42 (2008) 6959–6972

Contents lists available at ScienceDirect

Atmospheric Environment

journal homepage: www.elsevier.com/locate/atmosenv

Near real time monitoring of biomass burning particulate emissions (PM2.5) across contiguous United States using multiple satellite instruments

Xiaoyang Zhang [a,*], Shobha Kondragunta [b], Christopher Schmidt [c], Felix Kogan [b]

[a] Earth Resources Technology, Inc., NOAA/NESDIS/Center for Satellite Applications and Research, 5200 Auth Road, Camp Springs, MD 20746, USA
[b] NOAA/NESDIS/Center for Satellite Applications and Research, 5200 Auth Road, Camp Springs, MD 20746, USA
[c] Cooperative Institute for Meteorological Satellite Studies, University of Wisconsin, 1225 W. Dayton St., Madison, WI 53706, USA

ARTICLE INFO

Article history:
Received 17 October 2007
Received in revised form 22 March 2008
Accepted 18 April 2008

Keywords:
Biomass burning emissions
Particulate matter
Multiple satellite instruments
GOES
Near real time

ABSTRACT

Biomass burning is a major source of aerosols that affect air quality and the Earth's radiation budget. Current estimates of biomass burning emissions vary markedly due to uncertainties in biomass density, combustion efficiency, emission factor, and burned area. This study explores the modeling of biomass burning emissions using satellite-derived vegetative fuel loading, fuel moisture, and burned area across Contiguous United States (CONUS). The fuel loading is developed from Moderate-Resolution Imaging Spectroradiometer (MODIS) data including land cover type, vegetation continuous field, and monthly leaf area index. The weekly fuel moisture category is retrieved from AVHRR (Advanced Very High Resolution Radiometer) Global Vegetation Index (GVIx) data for the determination of fuel combustion efficiency and emission factor. The burned area is simulated using half-hourly fire sizes obtained from the GOES (Geostationary Operational Environmental Satellites) Wildfire Automated Biomass Burning Algorithm (WF_ABBA) fire product. By integrating all these parameters, quantities of PM2.5 (particulate mass for particles with diameter $<2.5\,\mu m$) aerosols are calculated for each individual fire at an interval of half hour from 2002–2005 across CONUS. The PM2.5 estimates indicate that the annual PM2.5 emissions are 3.49×10^5, 3.30×10^5, 1.80×10^5, and 2.24×10^5 tons for 2002 (April to December), 2003, 2004, and 2005, respectively. Among various ecosystems, forest fires release more than 44% of the emissions although the related burned areas only account for less than 30%. Spatially, PM2.5 emissions are larger in California for all these years, but only for some individual years in Oregon, Montana, Arkansas, Florida, Arizona, Louisiana, and Idaho. Finally, the calculated PM2.5 emissions are evaluated using national wildfire emission inventory data (NWEI) and compared with estimates from different fuel loadings. The difference between NWEI and GOES fire-based estimate is less than 20% if the same fuel data are used. The evaluation suggests that the biomass burning emissions derived from multiple satellite data provide realistic spatiotemporal patterns and can be assimilated into air quality models for forecasts in real or near real time.

© 2008 Elsevier Ltd. All rights reserved.

1. Introduction

Biomass burning releases trace gases (e.g., carbon monoxide (CO), carbon dioxide (CO_2), and methane (CH_4)) and aerosol emissions, which play a significant role in atmospheric chemistry. For example, it accounts for about

* Corresponding author. Tel.: +1 3017638346; fax: +1 3017638580.
E-mail address: xiaoyang.zhang@noaa.gov (X. Zhang).

1352-2310/$ – see front matter © 2008 Elsevier Ltd. All rights reserved.
doi:10.1016/j.atmosenv.2008.04.060

32% of CO and 40% of CO_2 released to the atmosphere globally (Levine, 1996). These emissions and their long-distance transports contribute significantly to the uncertainty in simulating climate change and global warming (Twomey, 1977). They also affect both local and global air quality which has strong impacts on human health and environmental pollution (Seiler and Crutzen, 1980; Phuleria et al., 2005; Sapkota et al., 2005). Currently, the aerosol emitted from biomass burning is one of the major sources of uncertainty in air quality forecasting using models such as the Community Multi-scale Air Quality (CMAQ) (Dennis et al., 1996; Byun and Schere, 2006; Eder and Yu, 2006), and is a critical air pollutant subject to the National Ambient Air Quality Standards (NAAQS) established by the United States (US) Environmental Protection Agency (EPA) (EPA, 2003).

The estimates of emissions released from biomass burning have emerged as an important research topic. Recently, Fire Radiative Power (FRP) has been retrieved from satellite observations as a proxy for emissions (Wooster and Zhang, 2004; Roberts et al., 2005; Ichoku and Kaufman, 2005). This method integrates temporal FRP over a fire event to measure the total Fire Radiative Energy (FRE), which is then converted into the total combusted biomass using statistical models. The FRE provides a great potential to estimate emissions directly although the uncertainty is currently high and the coefficients between FRE and emissions need to be well determined (Ichoku and Kaufman, 2005).

Emissions from biomass burning are primarily modeled using a set of parameters that includes fuel loading and burned area. Fuel loading is a complex parameter and the main source of uncertainty in emission estimates (Wiedinmyer et al., 2006). Because of the difficulty in parameterizing fuel loading, a variety of datasets have been used in emission modeling. The commonly used fuel loading datasets include static values at continental scales (Goode et al., 2000; Liu, 2004; Freitas et al., 2005), field measurements in local plot areas ($<100\ m^2$) (Trollope et al., 1996; Hoffa et al., 1999), estimates from terrestrial ecosystem models (Lü et al., 2006), and ecoregion-based representatives in regional areas (Soja et al., 2004; Reid et al., 2004; Wiedinmyer et al., 2006). The most widely used fuel data in Continuous United States (CONUS) are derived from National Fire Danger Rating System (NFDRS) (Deeming et al., 1977; Burgan et al., 1998), which are associated with fuel models using a lookup table. To improve the quality of NFDRS fuel data, a similar fuel dataset called the Fuel Characteristic Classification System (FCCS) has recently been developed by US Department of Agriculture Forest Service (Sandberg et al., 2001), and provides more detailed ecosystem types and fuel types. The quality of such fuel datasets depends greatly on the class schemes of ecoregions and the representatives of fuel values.

Burned area is another major parameter in emission modeling. In investigating historical fire emissions, the burned areas from wildland fires are usually derived from potential natural vegetation and ecological fire regime information (Leenhouts, 1998) and from local and national fire services or agencies (Hao and Liu, 1994; EPA, 2003; Lü et al., 2006). Recently, satellite observations have provided a means to monitor burned areas at a more accurate spatial pattern. As a result, fire (hotspot) counts from various satellites, such as the Along Track Scanning Radiometer (ATSR), the Advanced Very High Resolution Radiometer (AVHRR), and the Moderate-Resolution Imaging Spectroradiometer (MODIS), have been used as a proxy for the investigation of biomass burning (Eva and Lambin, 1998; Duncan et al., 2003; Wiedinmyer et al., 2006). Because of the challenge to link the fire counts to burned areas (Boschetti et al., 2004; Soja et al., 2004), burn scars are detected from satellites to analyze historical variations in biomass burning emissions (Hoelzemann et al., 2004); however, they are not able to be produced in near real time (Roy et al., 2002; Boschetti et al., 2004). Alternatively, Geostationary Operational Environmental Satellites (GOES) provide highly frequent measurements of fire occurrences (Prins et al., 1998). The fire pixels retrieved from GOES data have recently been associated with smoke and aerosol coverage (Prins et al., 1998), which is necessary to model the diurnal variation of smoke mass in the source region (Wang et al., 2006). The GOES instantaneous fire sizes have been demonstrated to be potentially useful in aerosol forecasting in near real time (Reid et al., 2004), but they differ from actual burned areas (Prins et al., 1998). Thus, the corresponding burned areas and fuel loadings need to be well quantitatively defined.

To support operational air quality forecasts, NOAA (National Oceanic and Atmospheric Administration) Air Quality program has requested NESDIS (National Environmental Satellite, Data, and Information Services) to develop near real time aerosol emissions from biomass burning events. For this purpose, we use multiple satellite instruments to retrieve spatially distributed parameters for the modeling of PM2.5 (particulate matter with diameters less than 2.5 μm) emissions across CONUS. Particularly, a new fuel dataset is developed from MODIS vegetation properties. Burned area is simulated from sub-pixel fire sizes obtained from GOES WF_ABBA (Wildfire Automated Biomass Burning Algorithm) fire product. Combustion and emission factors are associated with fuel moisture category derived from AVHRR vegetation health condition. The calculated PM2.5 emissions from 2002 to 2005 are examined in temporal and spatial patterns. Finally, the PM2.5 results are evaluated using different fuel loading datasets and national emission inventory.

2. Modeling biomass burning emissions

2.1. Model of biomass burning emissions

Emissions from biomass burning are controlled by four fundamental parameters. These parameters are burned area, fuel loading (biomass density), the fraction of combustion, and the factor of emissions for trace gases and aerosols. By integrating these parameters, Seiler and Crutzen (1980) have developed a standard formula to model the biomass burning emissions:

$$E = ABCF \tag{1}$$

where E represents the emissions from biomass burning (ton); A is the burned area (ha); B is the biomass density

(ton ha^{-1}); C is the fraction of biomass consumed during a fire event; and F is the factor of the consumed biomass released as trace gases and smoke particulates. This simple model has been widely used to estimate the emissions in regional and global scales (Ito and Penner, 2004; Reid et al., 2004; Soja et al., 2004; Korontzi, 2005; Wiedinmyer et al., 2006).

To accurately estimate the smoke particulates released from biomass burning, we employ the format of model (1) to calculate emissions at different temporal and spatial scales. It is due to the fact that fuel moisture condition varies in different time periods and burned area is a function of fire event and fire behavior. Moreover, these parameters are determined based on satellite pixels, which changes among pixels. Thus, the emission model is modified to the following format:

$$E = \sum_{k=1}^{K}\sum_{l=1}^{L}\sum_{j=1}^{J}\sum_{i=1}^{I} A_{ijk}B_{ijl}C_{ijkl}F_{ijkl} \tag{2}$$

where E is the particulate emissions in a certain time period and location (ton); i and j define the fire (pixel) location in column and row; l is the fuel type; k is the time period; A is the burned area (ha); B is the amount of fuel mass available for combustion (ton ha^{-1}); C is the combustion factor, and F is the emission factor for particle PM2.5.

The parameters for estimating biomass burning emissions are derived from various MODIS land surface products, AVHRR vegetation index data, and GOES fire data (Table 1). These parameters may vary with different time and space. The emission results are evaluated using other fuel-based estimates and national wildfire emission inventory (Table 1). The detailed procedure is described in the following sections.

2.2. Calculation of fuel loading

Fuel loading is basically divided into live and dead fuel loadings. The live fuel loading consists of canopy (foliage and branch) biomass in forests, shrub biomass, and grass (including crop) biomass, and the dead fuel loading is composed of litter and coarse woody detritus. To determine the fuel loadings for each pixel at a spatial resolution of 1 km, we developed a MODIS Vegetation Property-based Fuel System (MVPFS) using percent vegetation cover, leaf area index, and land cover types (Table 1). Percent vegetation cover, which includes tree cover, percent non-tree vegetation (shrubs, crop, and herbaceous), and percent bare ground, is derived from the MODIS vegetation continuous field (MOD44B) with a spatial resolution of 500 m (Hansen et al., 2003). Leaf area index (LAI) is obtained from the MODIS LAI product (MOD15A2) at a spatial resolution of 1 km and a temporal resolution of 8 days between 2001 and 2004 (Myneni et al., 2002), which is used to derive maxima monthly LAI. Land cover data are acquired from the MODIS land cover product at a 1 km resolution (Friedl et al., 2002).

Live fuel loading in forest foliage biomass and grass biomass is a function of percent vegetation cover, maxima monthly leaf area index, and land cover types. Specifically, foliage biomass and grass biomass are calculated using the specific leaf area (SLA) and LAI (Zhang and Kondragunta, 2006). The resultant foliage biomass in CONUS is less than 7 tons ha^{-1} in 90% of the forest areas mainly distributed in boreal forests and east coast regions (Fig. 1a), and the grass biomass is less than 5 tons ha^{-1} which is dominated in the central agriculture areas and western grassland and savanna regions (Fig. 1d). Branch biomass in forests is estimated using a generalized foliage-based allometric model (Zhang and Kondragunta, 2006). It is about 21 tons ha^{-1} on average and about 30 tons ha^{-1} in the regions of forest land cover types (Fig. 1b).

The total aboveground biomass for shrubs is a function of crown area or vegetation cover (Sah et al., 2004). To calculate shrub biomass, a regression model developed in the western US (Michell et al., 1987; Brown and Marsden, 1976; Chojnacky et al., 2004) is applied to CONUS.

$$B_s = 1.09 \times 10^5 - 2.161 \times 10^3\, V_c + 1.078 \times 10^2 V_c^2 \tag{3}$$

where B_s is the shrub biomass (kg km^{-2}) and V_c is the percentage of shrub cover. The resultant shrub biomass is high in the eastern US and the northwestern US while it is low in the open shrublands in the southern west US (Fig. 1c).

Employing the relationship of vegetation type with litter and coarse woody debris (CWD) developed by Matthews (1997), we generate a dataset of litter fuel loading and CWD at a 1 km resolution. The litter production is primarily composed of material such as leaves, fine wood, and fine roots, while coarse woody detritus is usually larger than 7 cm in diameter (Harmon et al., 1986). The pools of litter and CWD are investigated by compiling biomass density measurements for various vegetation types (Matthews, 1983, 1997; Ito and Penner, 2004). We reclassify the Matthews' vegetation types (Matthews, 1983) to MODIS IGBP (International Geosphere-Biosphere Programme) land cover types using a crosswalk rule. The corresponding litter and CWD data for each land cover type are then selected or averaged, separately.

To estimate litter and CWD more realistically, we separate percent vegetation cover for different land cover types in a 1-km pixel. Non-tree vegetation (percent) within the forest land cover types is assumed to be a mixture between

Table 1
Satellite and auxiliary data used for estimates of biomass burning emissions

Collected data	Resolution (space and time)	Purpose
MODIS land cover	1 km and static	Development of fuel loading
MODIS vegetation continuous field	0.5 km and static	Development of fuel loading
MODIS leaf area index	1 km and 8 days	Development of fuel loading
AVHRR global vegetation index	4 km and weekly	Determination of moisture condition
GEOS fire data	4 km and 30 min	Determination of burned area
NFDRS fuel data	1 km and static	Evaluation of model results
FCCS fuel data	1 km and static	Evaluation of model results
National wildfire emission inventory	Field point and daily	Evaluation of model results

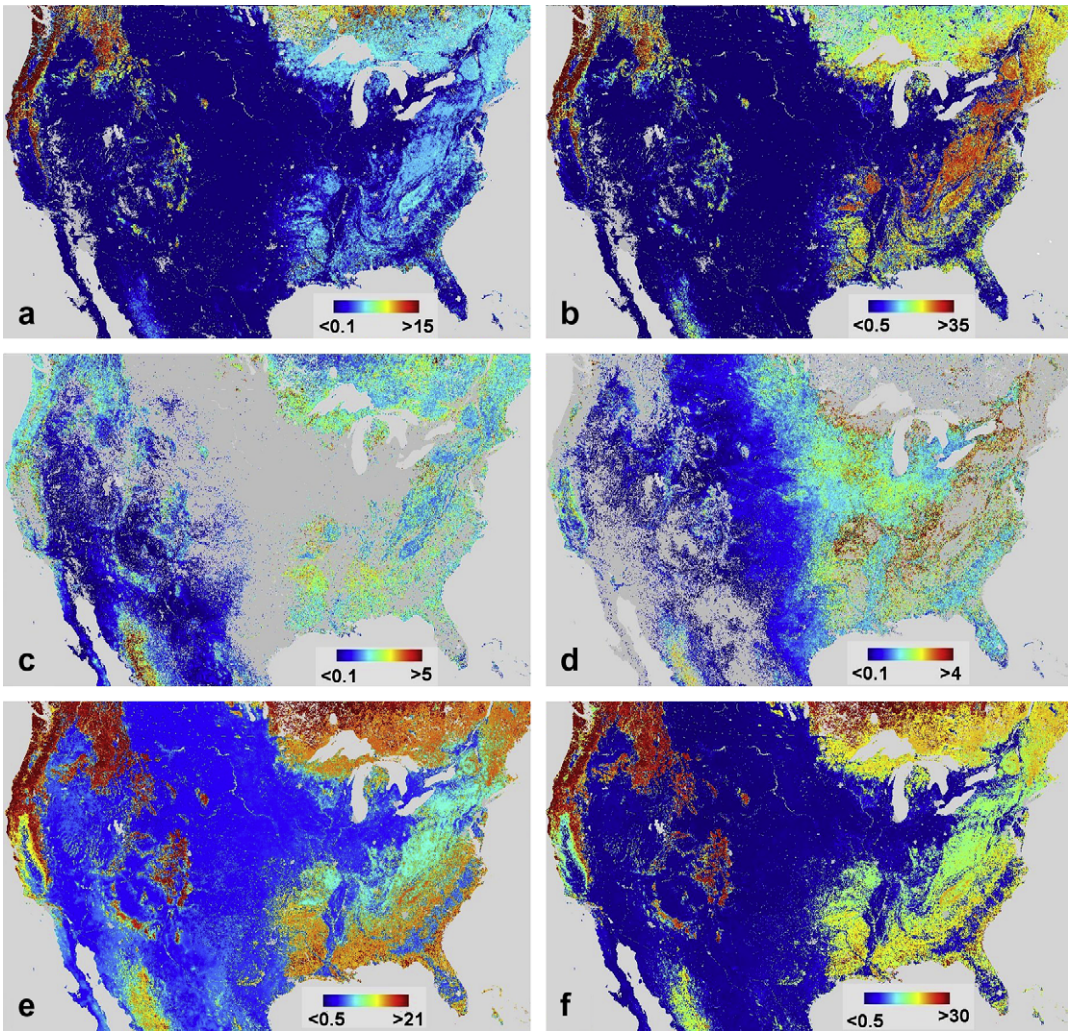

Fig. 1. Fuel loadings across CONUS (ton ha^{-1}). (a) Forest foliage, (b) forest branch, (c) shrub, (d) grass, (e) litter, (f) coarse woody detritus.

grasses and shrubs because they are not able to be further separated. On the other hand, the trees (percent) in the land cover types of non-forests are considered as mixed forests. Thus, the related litter and CWD in each pixel are refined using the following equation:

$$B_{\mathrm{lw}} = B_{\mathrm{lwf}} V_{\mathrm{cf}} + B_{\mathrm{lws}} V_{\mathrm{cs}} \tag{4}$$

where B_{lw} is litter or CWD density in a pixel (ton ha^{-1}); B_{lwf} and B_{lws} are litter or CWD density (ton ha^{-1}) for forests and non-forest vegetation, separately; V_{cf} and V_{cs} are percent tree (forest) cover and non-tree vegetation cover. The calculated litter and CWD are much larger in forests than in non-forest land cover regions (Fig. 1e and f). The CWD values are as high as 30 tons ha^{-1} in the northern needle leaf forests while the values are very small in the central agriculture areas. The litter displays a similar pattern but the values are relatively low.

2.3. Fire data and processing

NOAA GOES WF_ABBA produces a fire product from the GOES East and West data in an interval of half hour (Prins et al., 1998; Weaver et al., 2004). Particularly, the WF_ABBA detects instantaneous fires in sub-pixels using 3.9 and 10.7 μm infrared bands by assuming that the thermal radiance in a 4 km pixel is a linear mixture of radiance from a fire target and background (Matson and Dozier, 1981; Prins and Menzel, 1994). This fire product contains the time of fire detection, fire location in latitude and longitude, instantaneous estimate of sub-pixel fire size, and a quality flag (ranging from 0 to 5). The fire size is only retrieved for pixels with best quality (flag 0) but not for the fire pixels that are saturated and cloudy and that are indicated as high, medium, or low probability fires (flags 1–5). In the WF_ABBA product, the factors including clouds, extreme solar zenith angles, and satellite noise can obstruct the detections of some fire events and thus interrupt diurnal fire patterns. In this study, we acquire fire data from April

2002 to December 2005, which are retrieved from GOES-8 and 12 using WF_ABBA v6.0. Note that the updated fire data between January and March 2002 are not available.

We developed a set of models describing diurnal fire sizes to represent missed detections in temporal patterns. Analyzing the WF_ABBA fire product from 2002 to 2004 indicates that there are about two-third of the detected fires which are not quantified with sub-pixel fire size. Moreover, fires are not continuously detected in some large fire events. Therefore, fire sizes in these cases need to be replaced using simulated data. To do this, we select all half-hourly sub-pixel fire sizes from GOES fire data between 2002 and 2005, and separate those with land cover types. For each ecosystem, the fire sizes in each specified half hour are averaged to generate diurnal variations. The averaged values are then fitted using a Fourier model to create a set of representative curves of diurnal sub-pixel fire sizes for forests, savannas, shrublands, grasslands, and croplands, respectively (Zhang and Kondragunta, 2008). The diurnal patterns in various ecosystems are similar, which is largest around 13:00 local solar time (LST). The half-hourly fire size in shrublands and savannas is generally larger during 10:00–15:00 LST than other hours. The diurnal pattern is most distinctive in croplands where large fire size dominates during daytime. In contrast, the diurnal fire size in forests is relatively stable throughout a day. These patterns are comparable to those of satellite active fire counts obtained in various studies (Justice et al., 2002; Roberts et al., 2005; Giglio, 2007). The diurnal pattern is also associated with diurnal variations in fire weather conditions (Schroeder and Buck, 1970), fuel moisture (Rothermel and Mutch, 1986), fuel temperature (Countryman, 1966), and human activity (Giglio, 2007).

Using the representative diurnal curves, we simulate fire size and use it as a proxy for burned area. Specifically, we assume that the curve shape of the diurnal fire size for a specified ecosystem should be similar but the magnitude could be different for various GOES fire pixels (4 km). Thus, the representative diurnal curve for the related ecosystem is shifted to fit available GOES sub-pixel fire sizes in a pixel during previous 24 h (or previous day). Moreover, we assume that the fire was burning continuously in a given pixel during the first and last instantaneous observations because fire smokes and clouds could obstacle GOES Imager from detecting fires. In this algorithm, the fire sizes in fire pixels with flags 1–5 (about 60% of total observations) are obtained from fitted diurnal curves. However, if the fires are under clouds during the whole burning period and there are not any half-hourly GOES fire detections at all for a fire pixel, thus this fire pixel would be missed in near real time estimates. Fortunately, such fire events are generally very small and contribute limited burning emissions. The sub-pixel fire size in the diurnal curve is converted to the burned areas using the equation:

$$A = \alpha F \tag{5}$$

where A is the area burned within a specified time period (km^2), F is the sub-pixel fire size (km^2), and α is a constant coefficient.

To determine the coefficient in Eq. (5), we compare the cumulative simulated GOES fire sizes with 20 TM-based burn scars (obtained from http://burnseverity.cr.usgs.gov/) across CONUS in 2002. The results indicated that α can be set to 1 if the cumulative fire sizes are calculated as the following (Zhang and Kondragunta, 2008): (1) from the whole diurnal curve if the observed GOES fires in a fire pixel last longer than 14 h; (2) between first and last GOES detections along the corresponding fitted curve if the detected fire duration is short. The burned area generated with this procedure is well matched with the burn scars detected from Landsat TM imagery, where the two datasets are generally distributed along a 1:1 line (slope is 0.923) with a strongly significant correlation ($p < 0.0001$). The simulated GOES burned area also compares well to the burned area reported in NWEI data across CONUS (Zhang and Kondragunta, 2008). The data pairs in the grid size of 20 min reveal that the simulated GOES burned area accounts for 91% of the variation in the burned areas from NWEI. The total difference between them is about 15%.

2.4. Determination of combustion and emission factors

Combustion and emission factors are dependent on fuel type and moisture condition. We determine fuel moisture conditions from time series of AVHRR Global Vegetation Index (GVIx) data, which are then related to moisture category factors for estimating the factors of combustions and emissions.

2.4.1. Determination of fuel moisture conditions

Vegetation Condition Index (VCI) is employed as a surrogate to represent the fuel moisture conditions required for calculating the factors of combustions and emissions. The weekly VCI provided in the NOAA AVHRR product has been demonstrated to be effective in monitoring drought information for various environments (Kogan, 1995). This parameter is derived from the Normalized Difference Vegetation Index (NDVI) (Kogan, 1995, 1997):

$$\mathrm{VCI} = 100 \times \frac{\mathrm{NDVI} - \mathrm{NDVI}_{\min}}{\mathrm{NDVI}_{\max} - \mathrm{NDVI}_{\min}} \tag{6}$$

where $\mathrm{NDVI}_{\max}$ and $\mathrm{NDVI}_{\min}$ in a pixel are the maximum and minimum values, respectively, in the corresponding week from 1985 to 2005.

In this study, we obtain weekly VCI values from 2002 to 2005, which are produced from the NOAA Global Area Coverage (GAC) using smoothed weekly NDVI datasets at a spatial resolution of 4 km. The weekly VCI values ranging from 0 to 100 are equally divided into six different categories which represent fuel moisture conditions of very dry, dry, moderate, moist, wet, and very wet, respectively (Fig. 2). The weekly variation in moisture conditions is used to associate with fuel moisture category factors (mcf), which are discussed in the following section.

2.4.2. Factors of combustions and emissions

The factor of combustion is a function of fuel type and moisture category. The combustion factors are calculated from the following model (Anderson et al., 2004):

$$C_l = \left(1 - e^{-1}\right)^{\mathrm{mcf}} \tag{7}$$

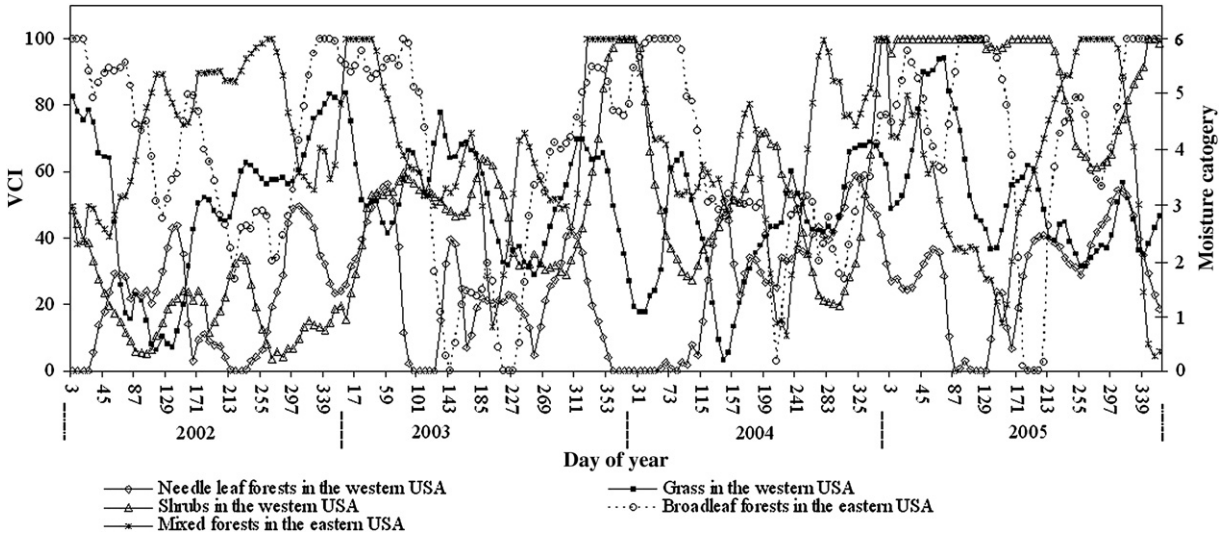

Fig. 2. Variation in fuel moisture category and VCI from 2002 to 2005. Moisture category is defined as very dry (0–1), dry (1–2), moderate (2–3), moist (3–4), wet (4–5), and very wet (5–6).

where C_l denotes the fraction of fuel loading consumed for fuel type l which is canopy (foliage and branch), shrub, and grass, separately; and mcf is the moisture category factor. The mcf value in each fuel type is determined using the fuel moisture condition derived from AVHRR VCI data (Table 2), which increases from dry to wet fuel conditions. As a result, C_l varies with the temporal (weekly) AVHRR VCI.

The fraction of combustion for litter is assumed to be 100% under various moisture conditions. This may overestimate biomass burning for the crown fires if the litter is not fully burned. However, the value for CWD is calculated using the following formula (Anderson et al., 2004):

$$C_w = 0.6(0.31 + (0.03 \times (0.31 - \mathrm{mcf}))) \quad (8)$$

The factor of PM2.5 emitted from the burned fuel loading also varies with fuel types and moisture conditions. We adopt the values from the Fire Order Fire Effects Model (Reinhardt et al., 1997). Thus, the emission factor for coarse wood is 8.10, 9.15, 11.25 kg Mg^{-1} for fuel moisture conditions of dry, moderate, and wet, respectively. However, the values of emission factors for litter, canopy, shrub, and grass are currently constant in various moisture conditions, which are 3.95, 10.65, 10.65, and 10.65 kg Mg^{-1}, respectively.

3. Methods of assessing PM2.5 emission estimates

3.1. Estimates of PM2.5 emissions from different fuel datasets

Because fuel loading is one of the main sources of uncertainties in estimating biomass burning emissions, we investigate the effects of fuel loadings on emission estimates by comparing our MVPFS-based results with emissions derived from the NFDRS and the FCCS fuel loadings. The NFDRS fuel map consists of 21 fuel models, and each fuel model is assigned with live and dead fuel loadings using a lookup table. The commonly used fuel model map is available at the US Forest Service (http://www.fs.fed.us/land/wfas/fuels/fdfuelmap.gif). Although the spatial resolution of the map is 1 km, it is derived from ecoregion polygons instead of individual pixels of vegetation properties. A polygon in NFDRS could cover several US sates, where same fuel value is assigned. This dataset is originally designed for the assessment of fire risks (Deeming et al., 1977), although it has been modified for estimating biomass burning emissions (Cohen and Deeming, 1985; Burgan et al., 1998; Leenhouts, 1998; Reinhardt et al., 1997). Relatively, the FCCS fuel dataset is more comprehensive, which separates live and dead fuel loadings as 16 types for 112 fuelbed types across CONUS (Sandberg et al., 2001). The fuelbed type in the FCCS data is classified using ecoregions, potential natural vegetation, and land use, and interpreted to 1 km resolution. The quantitative estimates of fuel loadings within the fuelbeds are derived from georeferenced stand-level data on the six ranger districts in forests. However, both the NFDRS and the FCCS datasets do not provide fuel information in agriculture areas. Further, fuel loading is assumed to be homogeneous in a large polygon region (which is much smaller in FCCS than in NFDRS dataset) and present sharp boundary between neighbor polygons (values). For example, difference of the fuel loadings can be demonstrated in Mcnally fire (36°3′N and 118°24′W) that occurred in July 2002 (Fig. 3). In this case,

Table 2
Moisture category factor (mcf) (from Anderson et al., 2004)

Moisture condition	Canopy	Shrub	Grass	Duff	CWD
Very dry	0.33	0.25	0.125	0.33	0.08
Dry	0.5	0.33	0.25	0.5	0.12
Moderate	1	0.5	1	1	0.15
Moist	2	1	2	2	0.22
Wet	4	2	4	4	0.31
Very wet	5	4	5	5	0.75

MVPFS fuel loading provides detailed spatial pattern (Fig. 3e) that is comparable with the TM-based vegetation distribution, while NFDRS only presents five different values (Fig. 3c).

Combining with simulated GOES burned areas, AVHRR VCI-based combustion and emission factors, the NFDRS and the FCCS fuel datasets are also used to calculate PM2.5 emissions from 2002 to 2005. These resultant half-hourly PM2.5 data are aggregated to daily data and then compared with MVPFS fuel-based PM2.5 estimates using the indices including coefficient of determination (R^2), root mean square (RMS) difference, and percent systematic RMS difference (SRMSD) (Willmott, 1981). The SRMSD is a measure of the linear bias between MVPFS fuel-based PM2.5 and other estimates using the following formula:

$$\mathrm{SRMSD} = \left[\frac{1}{n}\sum\left(\widehat{Y} - X\right)^2\right]^{1/2} \tag{9}$$

where $\widehat{Y}$ is the estimated values from correlation models between MVPFS fuel-based PM2.5 estimates and other fuel-based PM2.5 values, and X represents other fuel-based PM2.5 estimates, and n is the sample number based on number of days per year.

3.2. National wildfire emission inventory for the evaluation of GOES-based PM2.5 emissions

We further compare our emission estimates against the Inter-RPO 2002 National Wildfire Emission Inventory (NWEI). The NWEI PM2.5 data for 2002 have been developed by Air Sciences Inc and EC/R Inc using Seiler and Crutzen's (1980) emission model (WRAP, 2005). In the NWEI estimates of PM2.5, fire events are collected from federal and state records and county level data with specified location, calendar day, and fire size. Fuel loading for each fire event is derived from NFDRS fuel model (Deeming et al., 1977) and adjusted by adding duff, tree crowns, and regional composites. Combustion factor is static for each NFDRS model (WRAP, 2005).

To fully understand the uncertainties in satellite-derived emission estimates, the NWEI PM2.5 in 2002 are used to evaluate PM2.5 emissions derived from the

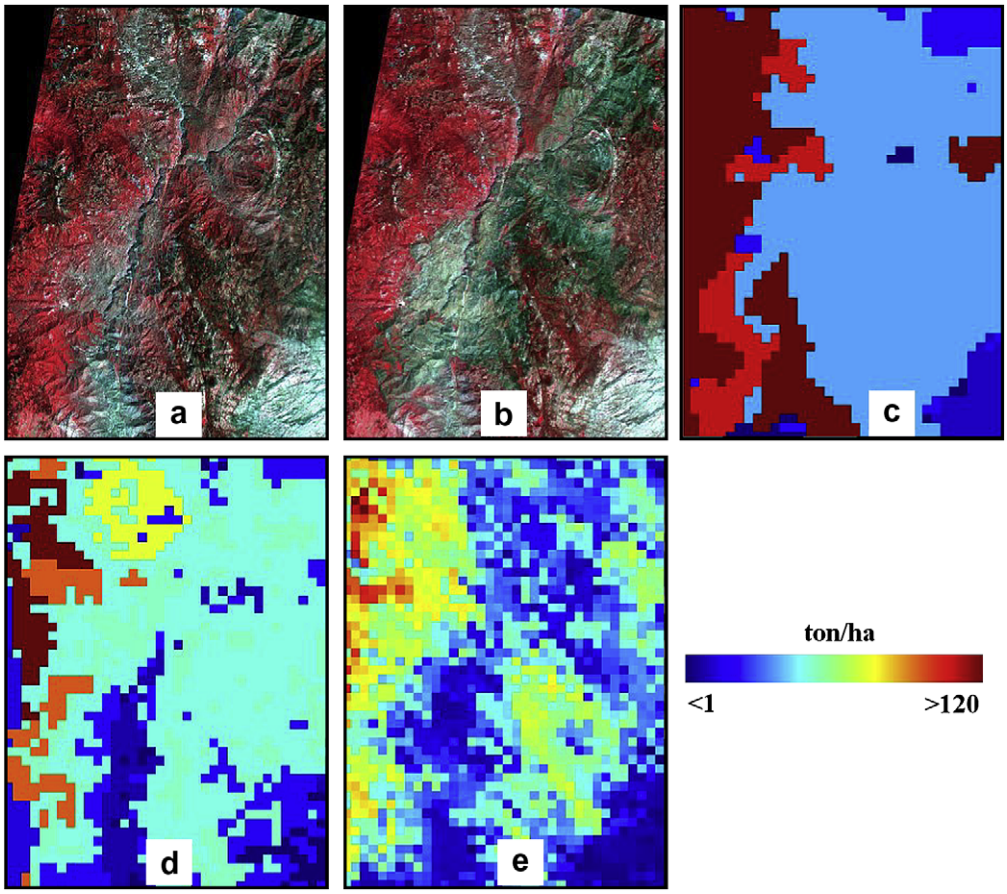

Fig. 3. Fuel loadings in the McNally area (35°49′–36°18′N, 118°10′–118°37′W), where fire occurred in July 2002. (a) Color TM composite (TM4-red, TM3-green, TM2-blue) before fire occurrence, where the red color indicates dense vegetation cover with large fuels and the grey and white colors represent sparsely vegetated areas with low fuels. (b) Color TM composite (TM4-red, TM3-green, TM2-blue) with spatial resolution of 30 m after fire occurrence, where the dark grey areas are burn scars. (c) Total NFDRS fuel loadings (1 km). (d) FCCS fuel loadings (1 km). (e) MVPFS fuel loadings (1 km), where the pattern is similar to the vegetation distributions in (a). Note that the TM imagery is obtained from the Joint NPS (National Park Service)–USGS (US Geological Survey) National Burn Severity Mapping Project (http://burnseverity.cr.usgs.gov/fire_main.asp).

simulated GOES burned areas. The latter are: (1) NFDRS-GOES: NFDRS fuels and static combustion and emission factors obtained from Cohen and Deeming (1985), which are close to the algorithm in NWEI except for the fire data; (2) FCCS-GOES-AVHRR: FCCS fuels and weekly-AVHRR-controlled emission and combustion factors; (3) MVPFS-GOES-AVHRR: MVPFS fuels and weekly-AVHRR-controlled emission and combustion factors. PM2.5 values for various estimates are matched up in 20 min grids across CONUS for comparison because it is difficult to match each fire event from the large amount of small fire events. This comparison excludes the grids where the fires are only detected in either GOES fire product or NWEI data. For three large fire events that covered more than one grid in the Hayman fire (105.42°W, 39.04°N, from June 8 to 28), the Rodeo fire (110.43°W, 34.09°N, from June 18 to July 3), and the fire in Oregon (123.94°W, 42.41°N, from July 14 to August 26), we match fire regions of the related fire events with a small buffer zone.

4. Results

4.1. PM2.5 emissions

The temporal and spatial patterns in PM2.5 estimates presented here are derived from MVPFS fuel loadings, simulated GOES burned areas (half-hourly), and weekly-AVHRR-controlled combustion and emission factors. The results aggregated from half-hourly estimates indicate that the annual PM2.5 emissions are 3.49×10^5, 3.30×10^5, 1.80×10^5, and 2.24×10^5 tons for 2002 (April–December), 2003, 2004, and 2005, separately. The large emissions are mainly distributed in the western US because large fire events occur often in the dry climate during summer season (Fig. 4). In contrast, the small emissions are spatially dense in the southeastern US overall the four years, where the emission values are relatively small while the occurrence of fire emissions is frequent, particularly in the areas around Kansas, Oklahoma, and Missouri. This is associated with prescribed agriculture fires which last only for a few hours or less in a day. However, PM2.5 emissions are sparsely dotted with small values in the central and northeastern US.

The PM2.5 emissions at a state level vary greatly (Fig. 5). The states with large proportions of the total annual emissions are Oregon (24.7%), California (13.8%), and Colorado (10.5%) in 2002; Montana (23.7%), California (12.8%), and Idaho (9.4%) in 2003; California (17.7%), Arizona (11.6%), and Florida (9.8%) in 2004; and Louisiana (10.2%), Idaho (9.0%), and Arkansas (7.5%) in 2005. To some extents, this spatial pattern is comparable with the simulated burned areas. The areas in California and Arizona account for more than 10% of the annual fires in CONUS from 2002 to 2005, separately. The other states with large burned areas are Oregon and Colorado in 2002, Montana and Idaho in 2003, Texas and Florida in 2004, and Texas and Louisiana in 2005. Evidently, the biomass burning emissions may

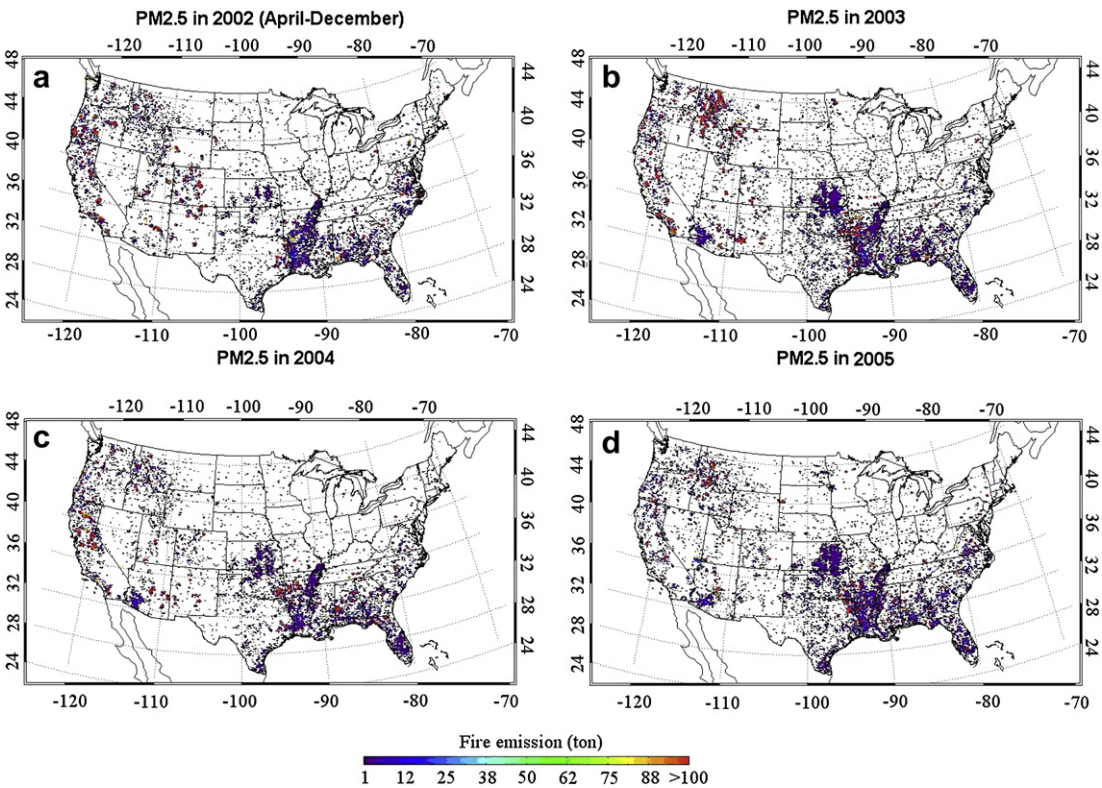

Fig. 4. Spatial patterns of annual PM2.5 emissions released from biomass burning in 2002 (a), 2003 (b), 2004 (c), and 2005 (d). Note that the dots increase with large values for display purpose.

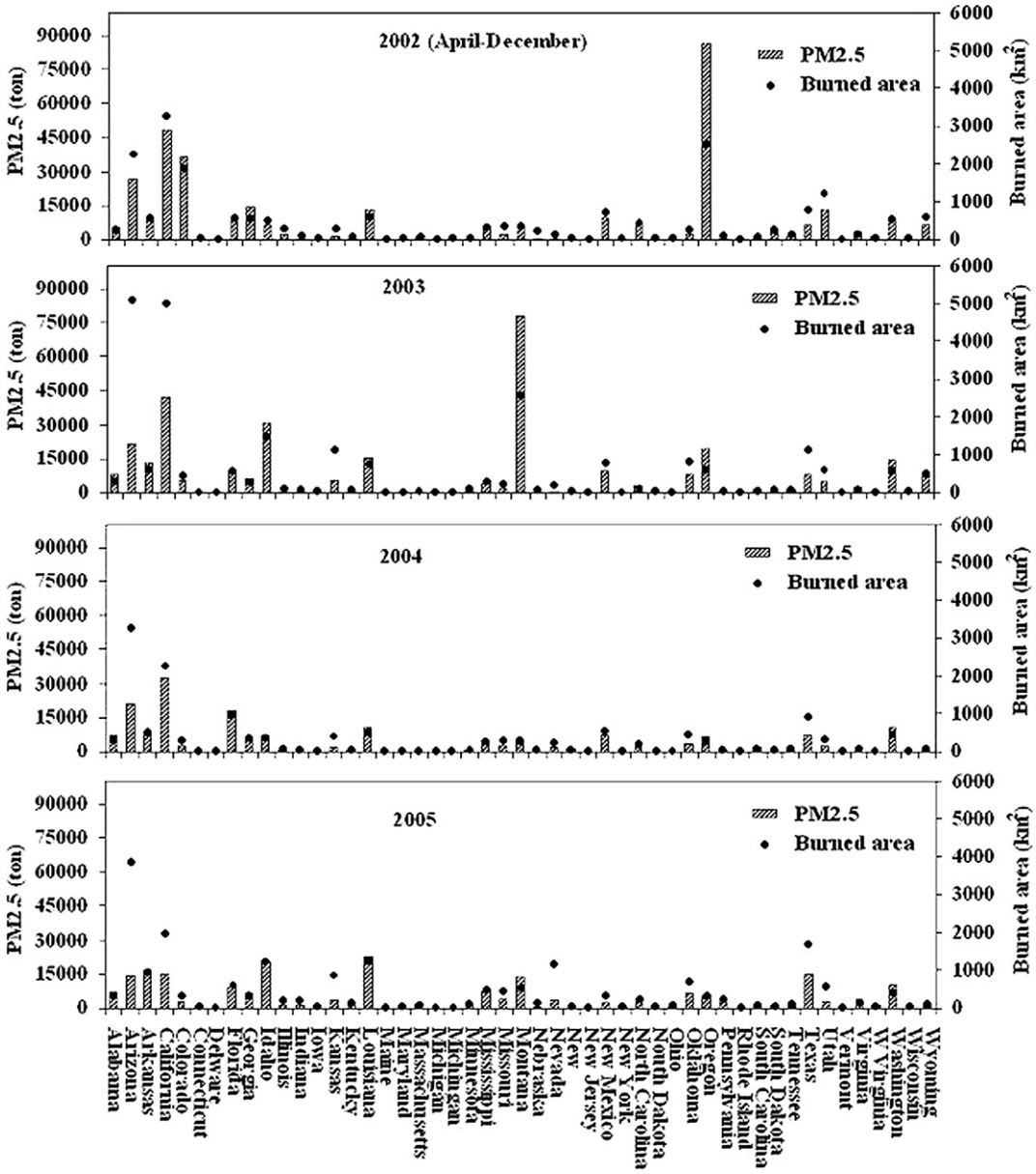

Fig. 5. Variations in PM2.5 emissions and simulated GEOS fire sizes in different states from 2002 to 2005.

have significant impacts on air quality in western and southeastern regions.

The magnitude of PM2.5 is also a function of ecosystem. The emissions are mainly released from forest fires (Fig. 6), which account for more than 44% of the annual amount during these four years. They are followed by those released from shrublands and savannas. Generally, these emissions are not correlated well with the burned areas in the corresponding land cover types. The simulated burned area in forests is less than 30% of the total burned areas, followed by those in shrublands, grasslands, agriculture areas, and savannas in 2002 and 2003 (Fig. 7). By contrast, the area is slightly larger in shrublands, but smaller in forests, croplands, grass, and savannas in 2004 and 2005.

The PM2.5 emission presents strong seasonal cycles (Fig. 8). The emissions in July and August account for more than 40% of the total annual amount while they are less than 10% from November to next February. The magnitude of this seasonality varies inter-annually, which is much stronger in 2002 and 2003 than in 2004 and 2005.

4.2. Effects of different fuel datasets on PM2.5 emission estimates

The daily PM2.5 emissions calculated from the MVPFS fuel data are significantly correlated with those calculated using the NFDRS and FCCS fuel loadings (Table 3). The high correlations exist between emissions derived from MVPFS

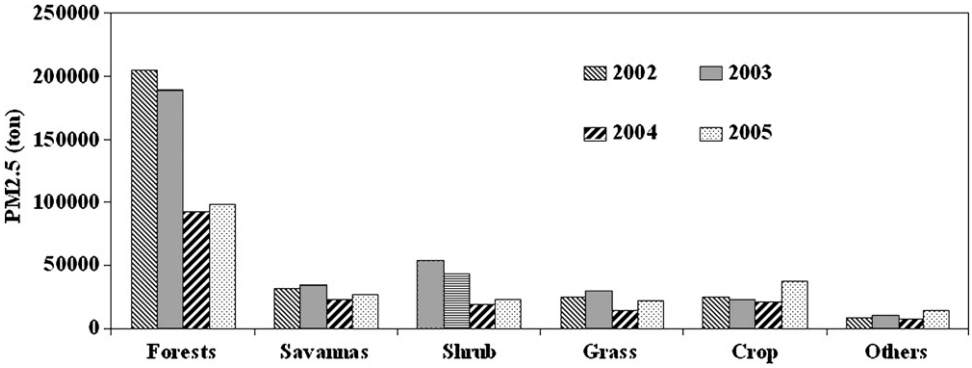

Fig. 6. PM2.5 emissions changing with land cover type.

and FCCS in 2002 and from MVPFS and NFDRS in 2003, 2004, and 2005. However, the magnitude of emissions from NFDRS fuel loadings is largest, which is about 30–50% higher than those from FCCS and MVPS fuel loadings. The emissions from MVPS fuel loading is about 17% larger than that from FCCS fuel in 2003, but about 7%, 1%, and 16% smaller in 2002, 2004, and 2005, separately. The large difference occurred in 2003 is associated with fuel data in west Montana where fire emission was largest at state levels. In this region, FCCS fuel loadings in the needle leaf forests are low relative to northwestern coast areas, while MVPFS fuel data (like the pattern in NFDRS fuel data) are similar in northwestern needle leaf forests. Overall, the RMS differences in daily emissions are smallest between MVPFS and FCCS, while the differences are large between MVPS and NFDRS for these years. Among these differences, the systematic differences between MVPFS and NFDRS, between MVPFS and FCCS, and between FCCS and NFDRS are 49–70%, 12–60%, and 44–71%, respectively. In other words, the unsystematic differences vary greatly among these fuel datasets. This comparison also demonstrates that the magnitudes of MVPFS-based and FCCS-based PM2.5 emissions are generally similar while they differ considerably from those calculated using NFDRS fuel loadings. This result suggests that MVPFS would be a realistic fuel data for the estimates of biomass burning emissions, because the FCCS data provide much more detailed fuel information relative to NFDRS data (Sandberg et al., 2001). On the other hand, the significant correlation between MVPFS-based emissions and NFDRS-based emissions indicates their good agreements in relative values.

4.3. Correlation between GOES PM2.5 emissions and NWEI data

The comparison between the matched data of PM2.5 emissions shows that three different emissions calculated from the simulated GOES burned areas all account for about 88% of variations in the NWEI PM2.5 emissions although the magnitude differs considerably (Fig. 9). Among the matched samples (grids, where about 28% of PM2.5 emissions in NWEI is excluded), the emission in the Rodeo fire event is much smaller in the GOES fire estimates than that in NWEI (the second largest value in Fig. 9a). It is likely associated with the fuel loadings used in NWEI because the simulated GOES burned area is similar to that from NWEI data (1035 km^2). Except for this sample, NFDRS-GOES estimates are very closely related to NWEI PM2.5 with samples distributed along a 1:1 line in the plot (Fig. 9) and a total difference is less than 20%. The small difference may be partially associated with the emission factors. The PM2.5 emission factors used in NWEI range from 11.36 to 16.62 kg Mg^{-1} (WRAP, 2005), while the values used in this study are 3.95–12.89 kg Mg^{-1} which are similar to other studies (e.g., Wiedinmyer et al., 2006). In contrast, the emissions from FCCS and MVPFS fuels (FCCS-GOES-AVHRR and MVPFS-GOES-AVHRR) are equivalently much smaller than NWEI PM2.5, especially in large fire events, which are

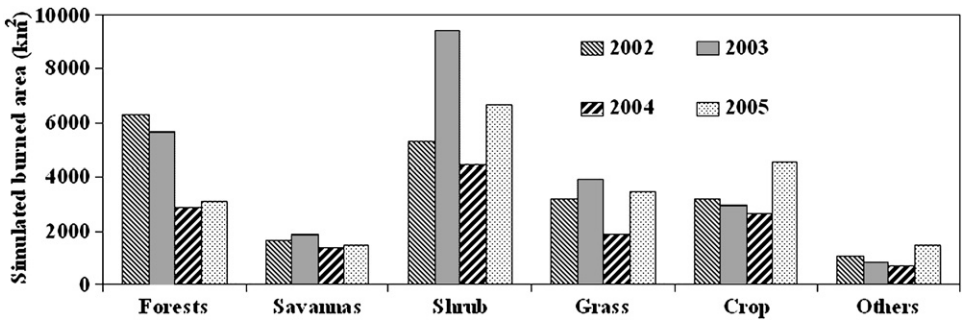

Fig. 7. Simulated GOES burned areas cumulated for different land cover types.

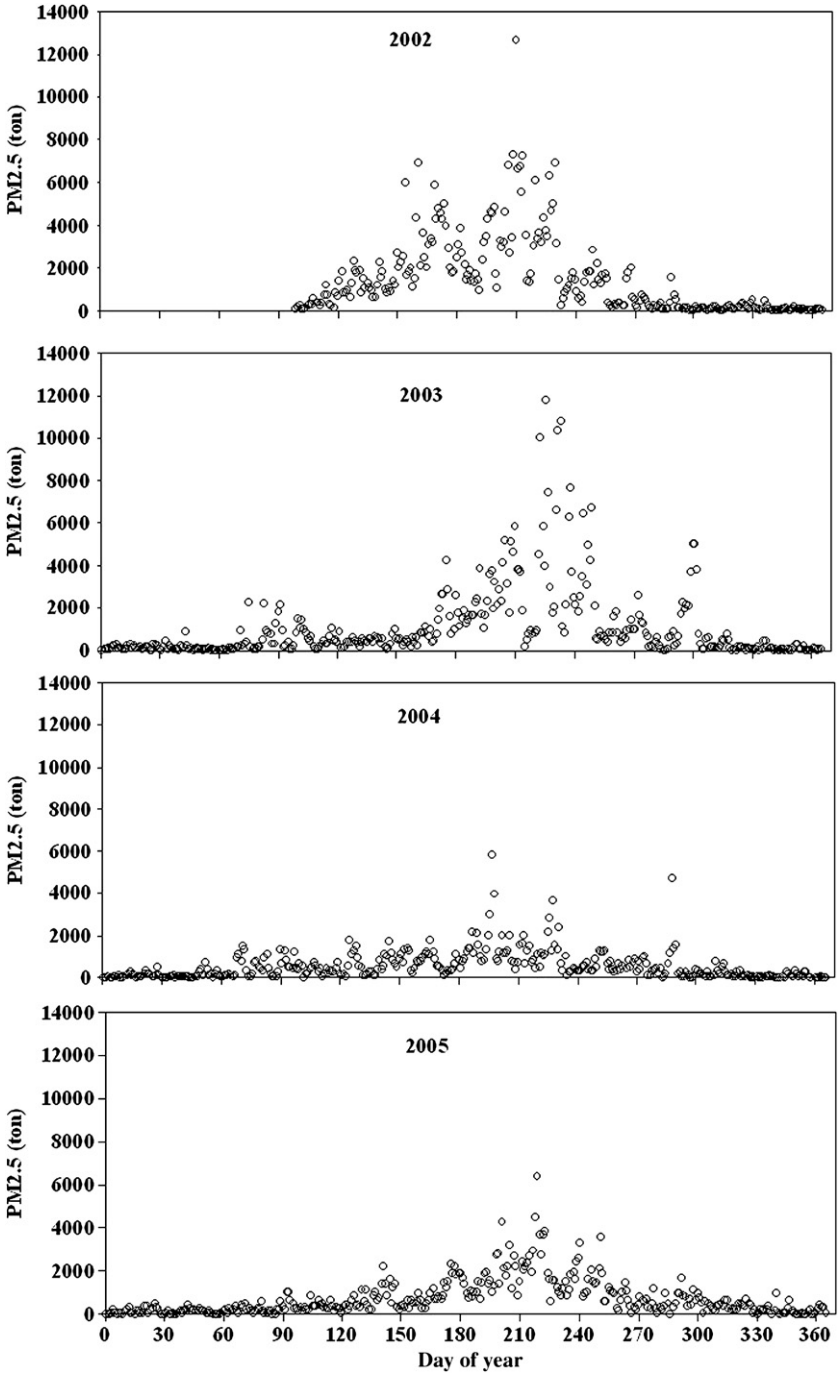

Fig. 8. Temporal variation in daily PM2.5 emissions cumulated from half-hourly biomass burning.

43% and 49% of NWEI values, respectively. This difference is likely due to the fact that NFDRS data assign a homogenously large fuel value to a large region while MVPFS and FCCS provide heterogeneous fuel data in each burned area.

5. Discussion and conclusions

PM2.5 emissions vary greatly with ecosystem, state, season, and year while the seasonal patterns are relatively stable. Fires and emissions mainly occur between June and August in CONUS. However, the magnitude of PM2.5 emissions varies in different years, which is much smaller in 2004 and 2005 than in 2002 and 2003. Although the burned areas in forests, shrublands and croplands are similarly large in all or some years, the emissions are mainly released from forest fires, which account for more than 44% of the total annual PM2.5 emissions. At the state level across CONUS, California always produces

Table 3
Statistical comparisons in daily emissions derived from different fuel loading datasets

	2002			2003			2004			2005		
	NFDRS	FCCS	MVPFS	NFDRS	FCCS	MVPFS	NFDRS	FCCS	MVPFS	NFDRS	FCCS	MVPFS
R^2												
NFDRS	1.00	0.836	0.889	1.000	0.722	0.922	1.000	0.694	0.840	1.000	0.621	0.803
FCCS	0.836	1.000	0.941	0.722	1.000	0.794	0.694	1.000	0.737	0.621	1.000	0.696
MVPFS	0.889	0.941	1.000	0.922	0.794	1.000	0.840	0.737	1.000	0.803	0.696	1.000
RMS (tons)												
NFDRS	0.00	2341	2252	0.00	2301	1383	0.00	744	590	0.00	817	652
FCCS	2341	0.00	457	2301	0.00	1065	744	0.00	352	817	0.00	477
MVPFS	2252	457	0.00	1383	1065	0.00	590	352	0.00	652	477	0.00
Percent of systematic RMS												
NFDRS	0.00	65.88	69.89	0.00	71.06	66.43	0.00	55.45	57.20	0.00	43.59	49.94
FCCS	65.88	0.00	13.30	71.06	0.00	60.92	55.45	0.00	23.80	43.59	0.00	12.17
MVPFS	69.89	13.30	0.00	66.43	60.92	0.00	57.20	23.80	0.00	48.94	12.17	0.00

NFDRS, FCCS, and NESDIS denote the emissions calculated using these three fuel datasets, respectively.

large amount of PM2.5 emissions every year. Other main sources of PM2.5 emissions in some individual years are Oregon, Montana, Florida, Arizona, Louisiana, Arkansas, and Idaho.

The PM2.5 estimated from GOES data are evaluated although direct validation is currently infeasible (Ito and Penner, 2004; Soja et al., 2004; Korontzi, 2005). First, comparing emissions from various fuel data demonstrates that the PM2.5 emissions estimated from MVPFS are reliable. Specifically, the PM2.5 estimated from NFDRS fuel loading is more than 35% larger relative to the values from both MVPFS and FCCS fuels. Giving the NFDRS fuel loadings are developed for assessing fire risk with homogenous values within large polygons (Burgan et al., 1998) while the FCCS fuels are dependant on much detailed ecosystem pattern (Sandberg et al., 2001), we believe that the FCCS fuel loading produces better PM2.5 estimates. Of course, future research is needed to better understand their differences using inter-comparison and reliable "truth" data. Further, the MVPFS and FCCS fuel loadings produce very similar PM2.5 estimates in both spatial and temporal patterns with an RMS difference less than 17%. This suggests that the MVPFS fuel loading can produce reasonable PM2.5 estimates. Moreover, MVPFS can easily be updated with land cover and land use changes and extended to other continents using latest satellite data while producing FCCS fuel data is highly time consuming and financial costs.

Second, the PM2.5 emissions calculated from GOES fire data match well with NWEI PM2.5 values if similar fuel loadings are used. The NWEI PM2.5 in 2002 is the best dataset currently available; nevertheless, this dataset itself is modeled from various parameters that contain large uncertainties. If we estimate PM2.5 using NFDRS fuel loadings and static combustion factors which are used in NWEI, and GOES fire data, the outputs are generally comparable to NWEI PM2.5 with a difference less than 20%. This suggests that the GOES fire dataset is a promise for emission calculations. From above evaluations, we can conclude that both GOES fire data and MVPFS fuel loadings are realistic in producing PM2.5 estimates.

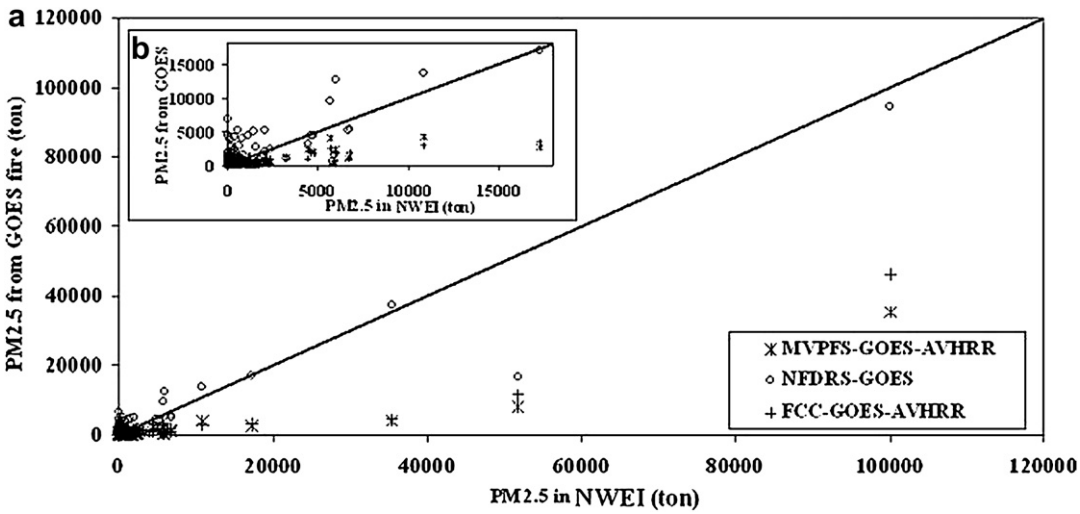

Fig. 9. Comparison of NWEI PM2.5 against estimates from simulated GOES burned areas and different fuel loadings in 2002 (April–December) (a). PM2.5 emissions are matched up in 20 min grids while the values in the three largest fire events are matched based on burn scars. The detailed information for small values is displayed in (b).

The overall uncertainty in PM2.5 estimates is roughly estimated from error propagations of inputs because of the lack of field PM2.5 measurements. Although the fuel loading is still a research issue (Kasischke and Penner, 2004), estimated uncertainties in the MVPFS fuel loadings are about 13% (Zhang and Kondragunta, 2006). Further, although the estimates of burned areas in large regions could differ greatly (Scholes and Andreae, 2000; Kasischke et al., 2003; Boschetti et al., 2004), the error of the simulated GOES burned areas is about 15% according to the comparison with national inventory data (Zhang and Kondragunta, 2008). Note that this error may be partially caused by understory fires because satellite sensors are generally unable to detect fires under dense tree canopy. Finally, the uncertainty of emission factors obtained from field measurements for many important species is about 20–30% (Andreae and Merlet, 2001). This value is assumed to be similar to that in combustion factor. Based on above uncertainties in the input parameters, the propagated error in our PM2.5 estimate could be as high as about 106%.

Overall, the multiple satellite-based algorithm developed in this study has several advantages for producing PM2.5 emissions in near real time. First, GOES WF_ABBA is monitoring fires in real time in NOAA/NESDIS and the fire product is available online (http://gp16.ssd.nesdis.noaa.gov/FIRE/fire.html). Using these instantaneous fire data, our algorithm simulates the diurnal fire sizes in representing burned areas in near real time. Second, AVHRR vegetation condition index (VCI) is operationally running in NOAA/NESDIS in near real time. The weekly VCI in previous week is employed in our algorithm to produce moisture conditions for determining dynamic combustion and emission factors. Finally, MVPFS fuel loading is pixel based rather than polygon based, which provides detailed spatial patterns. Therefore, by integrating these parameters, the PM2.5 emissions in near real time are currently produced in NOAA/NESDIS. We believe this algorithm is physically realistic although the results need to be thoroughly validated once reliable field data are available. Consequently, operationally running this algorithm in near real time can significantly contribute to the air quality forecasts, and can overcome some limitations in creating fire emissions inventories over large regions which are costly and time consuming.

Acknowledgments

This work was funded with support from NOAA Joint Center for Satellite Data Assimilation. We also wish to thank Don McKenzie for providing FCCS fuel loading dataset, and Wei Gou for providing AVHRR data. The views, opinions, and findings contained in these works are those of the author(s) and should not be interpreted as an official NOAA or US Government position, policy, or decision.

References

Anderson, G.K., Sandberg, D.V., Norheim, R.A., 2004. Fire Emission Production Simulator (FEPS) User's Guide (version 1.0). <http://www.fs.fed.us/pnw/fera/publications/fulltext/FEPS_User_Guide.pdf>.

Andreae, M.O., Merlet, P., 2001. Emission of trace gasses and aerosols from biomass burning. Global Biogeochemical Cycles 15 (4), 955–966.

Boschetti, L., Eva, H.D., Brivio, P.A., Grégoire, J.M., 2004. Lessons to be learned from the comparison of three satellite-derived biomass burning products. Geophysical Research Letters 31, L21501. doi:10.1029/2004GL021229.

Brown, J.K., Marsden, M.A., 1976. Estimating Fuel Weights of Grasses, Forbs, and Small Woody Plants. Research Note INT-210. US Department of Agriculture, Forest Service, Intermountain Forest and Range Experiment Station, Ogden, Utah. Available at: www.fs.fed.us/rm/main/pubs/inventories/int_rn/pdf, 11 pp.

Burgan, R.E., Klaver, R.W., Klaver, J.M., 1998. Fuel models and fire potential from satellite and surface observations. International Journal of Wildland Fire 8, 159–170.

Byun, D.W., Schere, K.L., 2006. Review of the governing equations, computational algorithms, and other components of the Models-3 Community Multiscale Air Quality (CMAQ) modeling system. Applied Mechanics Reviews 59, 51–77.

Chojnacky, D.C., Mickler, R.A., Meath, L.S., Woodall, C.W., 2004. Estimates of Down woody materials in eastern US forests. Environmental Management 33, S44–S55.

Cohen, J.D., Deeming, J.E., 1985. The National Fire Danger Rating System: Basic Equations. General Technical Report PSW-82. U.S. Department of Agriculture–Forest Service, Pacific Southwest Forest and Range Experiment Station, Berkeley, CA.

Countryman, C.M., 1966. The concept of fire environment. Fire Control Notes 27, 8–10.

Deeming, J.E., Burgan, R.E., Cohen, J.D., 1977. The National Fire-Danger Rating System – 1978 (General Technical Report INT-39). U.S. Department of Agriculture, Forest Service, Intermountain Forest and Range Experiment Station, Ogden, UT, 63 pp.

Dennis, R.L., Byun, D.W., Novak, J.H., Galluppi, K.J., Coats, C.J., Vouk, M.A., 1996. The next generation of integrated air quality modeling: EPA'S Models-3. Atmospheric Environment 30, 1925–1938.

Duncan, B.N., Martin, R.V., Staudt, A.C., Yevich, R., Logan, J.A., 2003. Interannual and seasonal variability of biomass burning emissions constrained by satellite observations. Journal of Geophysical Research 108 (D2), 4100. doi:10.1029/2002JD002378.

Eder, B., Yu, S., 2006. A performance evaluation of the 2004 release of Models-3 CMAQ. Atmospheric Environment 40, 4811–4824.

EPA, 2003. National Ambient Air Quality Standards (NAAQS). Research Triangle Park, NC, USA. <http://www.cpa.goviairs/criteria.htntl>.

Eva, H., Lambin, E.F., 1998. Burnt area mapping in Central Africa using ATSR data. International Journal of Remote Sensing 19 (18), 3473–3497.

Freitas, S., Longo, K., Silva Dias, M., Silva Dias, P., Chatfield, R., Prins, E., Artaxo, P., Grell, G., Recuero, F., 2005. Monitoring the transport of biomass burning emissions in South America. Environmental Fluid Mechanics 5, 135–167.

Friedl, A.F., McIver, D.K., Hodges, J.C.F., Zhang, X.Y., Muchoney, D., Strahler, A.H., Woodcock, C.E., Gopal, S., Schneider, A., Cooper, A., Baccini, A., Gao, F., Schaaf, C., 2002. Global land cover mapping from MODIS: algorithms and early results. Remote Sensing of Environment 83, 287–302.

Giglio, L., 2007. Characterization of the tropical diurnal fire cycle using VIRS and MODIS observations. Remote Sensing of Environment 108, 407–421.

Goode, J.G., Yokelson, R.J., Ward, D., Susott, R.A., Babbitt, R.E., Davies, M.A., Hao, W.-M., 2000. Measurements of excess O_3, CO_2, CH_4, C_2H_4, C_2H_2, HCN, NO, NH_3, HCOOH, CH_3COOH, HCHO, and CH_3OH in 1997 Alaskan biomass burning plumes by airborne Fourier transform infrared spectroscopy (AFTIR). Journal of Geophysical Research 105, 22,147–22,166.

Hansen, M.C., DeFries, R.S., Townshend, J.R.G., Carroll, M., Dimiceli, C., Sohlberg, R.A., 2003. Global percent tree cover at a spatial resolution of 500 meters: first results of the MODIS vegetation continuous field algorithm. Earth Interactions 7, 1–15.

Hao, W.M., Liu, M.H., 1994. Spatial and temporal distribution of tropical biomass burning. Global Biogeochemical Cycles 8, 495–504.

Harmon, M.E., Franklin, J.F., Swanson, F.J., Sollins, P., Gregory, S.V., Lattin, J.D., Anderson, N.H., Cline, S.P., Aumen, N.G., et al., 1986. Ecology of coarse woody debris in temperate ecosystem. Advances in Ecological Research 15, 133–302.

Hoelzemann, J.J., Schultz, M.G., Brasseur, G.P., Granier, C., 2004. Global wildland fire emission model (GWEM): evaluating the use of global area burnt satellite data. Journal of Geophysical Research 109, D14S04. doi:10.1029/2003JD003666.

Hoffa, E.A., Ward, D.E., Hao, W.M., Susott, R.A., Wakimoto, R.H., 1999. Seasonality of carbon emissions from biomass burning in a Zambian savanna. Journal of Geophysical Research-Atmospheres 104 (D11), 13841–13853.

Ichoku, C., Kaufman, Y.J., 2005. A method to derive smoke emission rates from MODIS fire radiative energy measurements. IEEE Transactions on Geoscience and Remote Sensing 43, 2636–2649.

Ito, A., Penner, J.E., 2004. Global estimates of biomass burning emissions based on satellite imagery for the year 2000. Journal of Geophysical Research 109, D14S05. doi:10.1029/2003JD004423.

Justice, C.O., Giglio, L., Korontzi, S., Owens, J., Morisette, J.T., Roy, D., Descloitres, J., Alleaume, S., Petitcolin, F., Kaufman, Y., 2002. The MODIS fire products. Remote Sensing of Environment 83, 244–262.

Kasischke, E.S., Penner, J.E., 2004. Improving global estimates of atmospheric emissions from biomass burning. Journal of Geophysical Research 109, D14S01. doi:10.1029/2004JD004972.

Kasischke, E.S., Hewson, J., Stocks, B.J., van der Werf, G., Randerson, J., 2003. The use of ATSR active fire counts for estimating relative patterns of biomass burning – a study from the boreal forest region. Geophysical Research Letters 30 (18), 1969. doi:10.1029/2003GL017859.

Kogan, F.N., 1995. Application of vegetation index and brightness temperature for drought detection. Natural Hazards: Monitoring And Assessment Using Remote Sensing Technique Advances In Space Research 15 (11), 91–100.

Kogan, F.N., 1997. Global drought watch from space. Bulletin of the American Meteorological Society 78 (4), 621–636.

Korontzi, S., 2005. Seasonal patterns in biomass burning emissions from southern African vegetation fires for the year 2000. Global Change Biology 11 (10), 1680–1700.

Levine, J.S., 1996. Biomass Burning and Global Change. The MIT Press, Cambridge, MA.

Leenhouts, B., 1998. Assessment of biomass burning in the coterminous United States. Conservation Ecology 2 (1), 1–24.

Liu, Y., 2004. Variability of wildland fire emissions across the contiguous United States. Atmospheric Environment 38, 3489–3499.

Lü, A., Tian, H., Liu, M., Liu, J., Melillo, J.M., 2006. Spatial and temporal patterns of carbon emissions from forests in China from 1950 to 2000. Journal of Geophysical Research 111, D05313. doi:10.1029/2005JD006198.

Matson, M., Dozier, J., 1981. Identification of subresolution high temperature sources using a thermal IR sensor. Photogrammatic Engineering and Remote Sensing 47, 1311–1318.

Matthews, E., 1997. Global litter production, pool, and turnover times: estimates from measurement data and regression models. Journal of Geophysical Research 102 (D15), 18,771–18,800.

Matthews, E., 1983. Global vegetation and land use: new high-resolution data bases for climate studies. Journal Climatic Applied Meteorology 22, 474–487.

Michell, J.E., Bartling, P.N.S., O'Brien, R.O., 1987. Understory cover–biomass relationship in the Front Range ponderosa pine zone. Research Notie RM-471. US Department of Agriculture. Forest Service, Rocky Mountain Forest and Range Experiment Station, Fort Collins, CO. Available at: www.fs.fed.us/rm/main/pubs/inventories/rm_rn.pdf, 5 pp.

Myneni, R.B., et al., 2002. Global products of vegetation leaf area and fraction absorbed PAR from year one of MODIS data. Remote Sensing of Environment 83, 214–231.

Phuleria, H.C., Fine, P.M., Zhu, Y.F., Sioutas, C., 2005. Air quality impacts of the October 2003 Southern California wildfires. Journal of Geophysical Research 110 (D7), D07S20. doi:10.1029/2004JD004626.

Prins, E.M., Menzel, W.P., 1994. Trends in South American biomass burning detected with the GOES visible infrared spin scan radiometer atmospheric sounder from 1983 to 1991. Journal of Geophysical Research 99 (D8), 16,719–16,735.

Prins, E.M., Feltz, J.M., Menzel, W.P., Ward, D.E., 1998. An overview of GOES-8 diurnal fire and smoke results for SCAR-B and 1995 fire season in South America. Journal of Geophysical Research 103 (D24), 31,821–31,835.

Reid, J.S., Prins, E.M., Westphal, D.L., Schmidt, C.C., Richardson, K.A., Christopher, S.A., Eck, T.F., Reid, E.A., Curtis, C.A., Hoffman, J.P., 2004. Real-time monitoring of South American smoke particle emissions and transport using a coupled remote sensing/box-model approach. Geophysical Research Letter 31, L06107. doi:10.1029/2003GL018845.

Reinhardt, E.D., Keane, R.E., Brown, J.K., 1997. First Order Fire Effects Model: FOFEM 4.0, User's Guide (General Technical Report INT-GTR-344). U.S. Department of Agriculture, Forest Service, Intermountain Research Station, Ogden, UT, 65 pp.

Roberts, G., Wooster, M.J., Perry, G.L.W., Drake, N., Rebelo, L.M., Dipotso, F., 2005. Retrieval of biomass combustion rates and totals from fire radiative power observations: application to southern Africa using geostationary SEVIRI imagery. Journal of Geophysical Research 110, D21111. doi:10.1029/2005JD006018.

Rothermel, R.C., Mutch, R.W., 1986. Behavior of the life-threatening Butte Fire: August 27–29, 1985. Fire Manage Notes 47 (2), 14–24.

Roy, D.P., Lewis, P.E., Justice, C.O., 2002. Burned area mapping using multitemporal moderate spatial resolution data - a bi-directional reflectance model-based expectation approach. Remote Sensing of Environment 83, 263–286.

Sah, J.P., Ross, M.S., Koptur, S., Snyder, J.R., 2004. Estimating aboveground biomass of broadleaved woody plants in the understory of Florida Keys pine forests. Forest Ecology and Management 203, 319–329.

Sandberg, D.V., Ottmar, R.D., Cushon, G.H., 2001. Characterizing fuels in the 21st Century. International Journal of Wildland Fire 10, 381–387.

Sapkota, A., Symons, J.M., Kleissl, J., Wang, L., Parlange, M.B., Ondov, J., Breysse, P.N., Diette, G.B., Eggleston, P.A., Buckley, T.J., 2005. Impact of the 2002 Canadian forest fires on particulate matter air quality in Baltimore City. Environmental Science and Technology 39, 24–32.

Scholes, M., Andreae, M.O., 2000. Biogenic and pyrogenic emissions from Africa and their impact on the global atmosphere. Ambio 29, 23–29.

Schroeder, M.J., Buck, C.C., 1970. Fire weather—a guide for application of meteorological information to forest fire control operations. Agricture Handbook 360. U.S. Department Agriculture, Washington, DC, 229 pp.

Seiler, W., Crutzen, P.J., 1980. Estimates of gross and net fluxes of carbon between the biosphere and the atmosphere from biomass burning. Climatic Change 2, 207–247.

Soja, A.J., Sukhinin, A.I., Cahoon, D.R., Shugart, H.H., Stackhouse, P.W., 2004. AVHRR-derived fire frequency, distribution and area burned in Siberia. International Journal of Remote Sensing 25, 1939–1960.

Trollope, W.S.W., Trollope, L.A., Potgieter, A.F.L., Zambatis, N., 1996. SAFARI-92 characterization of biomass and fire behavior in the small experimental burns in the Kruger National Park. Journal of Geophysical Research 101 (D19), 23531–23539.

Twomey, S., 1977. The influence of pollution on the shortwave albedo of clouds. Journal of Atmospheric Science 34, 1149–1152.

Wang, J., Christopher, S.A., Nair, U.S., Reid, J.S., Prins, E.M., Szykman, J., Hand, J.L., 2006. Mesoscale modeling of Central American smoke transport to the United States, 1: "top-down" assessment of emission strength and diurnal variation impacts. Journal of Geophysical Research 11, D05S17. doi:10.1029/2005JD006416.

Weaver, J.F., Lindsey, D., Bikos, D., Schmidt, C.C., Prins, E., 2004. Fire detection using GOES rapid scan imagery. Weather and Forecasting 19, 496–510.

Wiedinmyer, C., Quayle, B., Geron, C., Belote, A., McKenzie, D., Zhang, X., O'Neill, S., Wynne, K.K., 2006. Estimating emissions from fires in North America for air quality modeling. Atmospheric Environment 40, 3419–3432.

Willmott, C.J., 1981. On the validation of modes. Physical Geography 2, 184–194.

Wooster, M.J., Zhang, Y.H., 2004. Boreal forest fires burn less intensely in Russia than in North America. Geophysical Research Letters 31, L20505, doi:10.1029/2004GL020805.

WRAP, 2005. Inter-RPO National 2002 Wildfire Emissions Inventory – Final Work Plan, Air Sciences &EC/R. Project No. 178-7.

Zhang, X., Kondragunta, S., 2006. Estimating forest biomass in the USA using generalized allometric model and MODIS land data. Geographical Research Letter 33, L09402. doi:10.1029/2006GL025879.

Zhang, X., Kondragunta, S., 2008. Temporal and spatial variability in biomass burned areas across the USA derived from GOES fire product. Remote Sensing of Environment 112, 2886–2897.